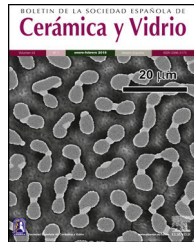




BOLETIN DE LA SOCIEDAD ESPAÑOLA DE  
**Cerámica y Vidrio**

[www.elsevier.es/bsecv](http://www.elsevier.es/bsecv)



## Chemical composition and alteration processes of glasses from the Cathedral of León (Spain)



Teresa Palomar<sup>a,b</sup>

<sup>a</sup> Unidade de Investigação VICARTE “Vidro e Cerâmica para as Artes”, FCT-UNL, Caparica, Portugal

<sup>b</sup> Instituto de Historia, CCHS-CSIC, Madrid, Spain

### ARTICLE INFO

#### Article history:

Received 25 June 2017

Accepted 9 October 2017

Available online 28 October 2017

#### Keywords:

Stained glass windows

Atmospheric weathering

Alteration pathologies

Cathedral of León

### ABSTRACT

The Cathedral of León has one of the most important ensembles of medieval stained glass windows in Europe; however, most of them have been altered by atmospheric weathering. The main objective of this study was the characterization of a set of glass samples from the Cathedral of León, the comparison with glasses from previous interventions in the cathedral and the study of the relation between the alteration pathologies, the chemical composition of the glasses and the environment in which they were placed. The samples were characterized by means of binocular microscopy, scanning electron microscopy and energy dispersive X-ray spectrometry, visible spectrophotometry, X-ray fluorescence spectrometry and X-ray diffraction. The main alteration of glasses exposed until the 19th century was the formation of pits by dealkalinization, while the glasses exposed until the present formed  $\text{CaSO}_4$  deposits as a consequence of the synergic effect of rainwater and gaseous pollutants. Glasses altered by the browning of manganese were also characterized.

© 2017 SECV. Published by Elsevier España, S.L.U. This is an open access article under the CC BY-NC-ND license (<http://creativecommons.org/licenses/by-nc-nd/4.0/>).

### Composición química y procesos de alteración de los vidrios de la Catedral de León (España)

### RESUMEN

La Catedral de León posee una de las colecciones de vidrieras medievales más importantes de Europa; sin embargo, muchos de los vidrios se han alterado por degradación atmosférica. El objetivo principal de este estudio fue la caracterización de un conjunto de vidrios procedentes de la Catedral de León, su comparación con vidrios procedentes de intervenciones previas en la catedral y el estudio de la relación entre las patologías de alteración, la composición química del vidrio y el medio en el que estuvieron expuestas. Las muestras se caracterizaron mediante lupa binocular, microscopía electrónica de barrido y microanálisis de dispersión de energía de rayos X, espectrofotometría visible, espectrometría de fluorescencia de rayos X y difracción de rayos X. La alteración principal de los vidrios expuestos

#### Palabras clave:

Vidrieras

Alteración atmosférica

Patologías de alteración

Catedral de León

hasta el s. XIX consistió en la formación de picaduras por desalcalinización, mientras que en los vidrios expuestos hasta la actualidad se formaron depósitos de  $\text{CaSO}_4$  como consecuencia del efecto sinérgico de la lluvia y los gases contaminantes. También se han caracterizado vidrios alterados por el enmarronamiento del manganeso.

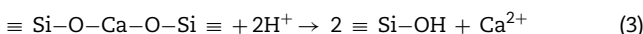
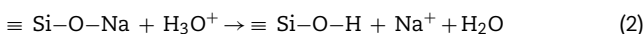
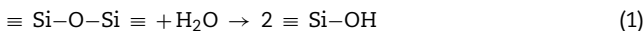
© 2017 SECV. Publicado por Elsevier España, S.L.U. Este es un artículo Open Access bajo la licencia CC BY-NC-ND (<http://creativecommons.org/licenses/by-nc-nd/4.0/>).

## Introduction

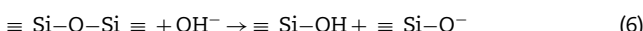
Glasses from stained glass windows are vulnerable to atmospheric environment because they are usually located in the building façades without protection. The outdoor surface of these glasses usually presents an intense alteration due to the exposition to rainwater, environmental pollution, temperature changes, wind-blown materials and bird droppings, among other factors. The most altered glasses were found in medieval stained glass windows, in which potash lime silicate glasses were used. As is known these glasses present low chemical stability [1,2].

The most common alteration process in atmospheric environment is soiling, which concerns the deposit of soot particles and soluble salts upon the glass surface. The most usual chemical species in soiling layers are sulfates, carbonates, nitrates and organic matter [3–5], from anthropic, biogenic, terrigenous or marine origin [6,7]. The main consequence of soiling is the diminishing of glass transparency, the change of roughness and the increasing of hygroscopicity [8].

The most common alteration pathology in glasses from stained glass windows are pits. The presence of water, from rain or condensation, on the glass surface can induce the glass network to break down (Reaction (1)) and the lixiviation of alkaline and alkaline-earth ions (Reaction (2) and (3)) [9].

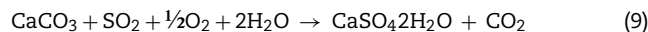
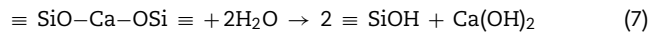


If water drops remain in stationary state upon the glass surface, a more intense corrosion process could occur. The  $\text{OH}^-$  ions formed on the surface (Reactions (4) and (5)) increase the pH of the hydration layer, which induces the breakdown of the glass network (Reaction (6)).



The lixiviated alkaline and alkaline-earths ions due to the hydrolytic attack ( $\text{K}^+$ ,  $\text{Na}^+$ ,  $\text{Ca}^{2+}$ , etc.) can react with the atmospheric pollutants contained in the environmental humidity ( $\text{CO}_2$ ,  $\text{SO}_2$ ,  $\text{NO}_x$ ) (Reactions (7)–(9)) and form deposits upon the glass surface and into the glass fissures [10–13]. The most common salts are sulfates, mainly gypsum ( $\text{CaSO}_4 \cdot 2\text{H}_2\text{O}$ )

and syngenite ( $\text{K}_2\text{Ca}(\text{SO}_4)_2 \cdot \text{H}_2\text{O}$ ); carbonates such as calcite ( $\text{CaCO}_3$ ); and oxalates ( $\text{CaC}_2\text{O}_4 \cdot n\text{H}_2\text{O}$ ) usually connected with biodeterioration processes [14–16].



Darkening, browning or blackening of the glass surface is a less common pathology. This phenomenon commonly occurs in the glass fragments used to represent the human skin, such faces or hands [17]. The pathology is characterized by the presence of dark opaque stains with high contents of  $\text{MnO}_2$ , both in the glass surface and in the corrosion crust [18]. These stains can affect severely the iconography of the stained glass windows, which could lose their original meaning and even diminish its artistic value [19].

The Cathedral of León has one of the most important collections of stained glass windows in Europe. The ensemble is formed by at about  $1800 \text{ m}^2$  of stained glass windows that compose 31 tall windows in the Central Nave and the Transept, three giant rose windows, ten medium windows in the lateral aisles, 15 windows in the chapels of the ambulatory, three large windows in the Santiago (Saint James) Chapel and small windows between the towers, the sacristy and the access to the cathedral cloister [20,21]. Most of the original stained glass windows are dated between the 13th and the 15th centuries. During the 13th century the main master glaziers were Pedro Guillermo and Juan Pérez; in the 14th century Diego de Santillana elaborated the stained glass windows from Santiago Chapel, and Rodrigo de Herreras the three windows from the Virgen Blanca (White Virgin) chapel. In the 15th century, Joaquín de Arquer and Alfonso Díez Anequín, among others, led a period of great artistic activity [20,22,23]. However, during the next years, the building was falling into a ruin state. At the end of the 19th century, the Spanish Government decided to close the cathedral and to carry out one of the most important restoration plans of the building, which also included the stained glass windows [20]. The work was led by the architect Demetrio de los Ríos and afterwards by Juan Bautista Lázaro. During the restoration of the stained glass windows the main criterion was the unity of style. Those original glasses which could not be reintegrated were saved in the Glassman boxes, where they were kept until nowadays [21]. After the restoration, the building was re-opened in 1901.

From 1993 to 2013 a new comprehensive restoration of the stained glass windows has been carried out in the Cathedral of León in the framework of programs such as “Salvemos nuestra Catedral” and “El sueño de la luz” [23]. Due to the long period

of restoration, several studies were developed on historical glasses [12,24–26], grisailles [27], metallic elements from the windows [28] and the putty corrosion products [29].

The main objective of this work was the characterization of a set of samples from the Cathedral of León, oriented to include it in a comprehensive study of the historical evolution of the chemical composition of the glasses from the cathedral, and to relate their chemical composition with the alteration pathologies found on the surface of glasses.

## Experimental

### Sample description

A set of 11 glass samples from the Cathedral of León were analyzed. They come from three different stained glass windows (Fig. 1) and from the Glassman boxes (Table 1). Two samples had undetermined location.

The fragment L1 came from the window nII, which is located in the North façade and represents vegetal and animal decoration; the glass fragment L2 came from the window I, located in the main chapel, which represents the Árbol de Jesse (Tree of Jesse), the genealogic tree of Christ from Jesse of Bethlehem, the father of the King David; and the samples L3–L7 came from the window SV, with representations of Priests and Prophets [21]. All the fragments are medieval glasses, except sample L11, which is a Renaissance glass.

Three samples (L3, L6 and L8) were flash glasses, formed by two layers of different color and thickness (Table 1), and four samples (L4–L7) were small fragments cut from the edges of the original glass during their restoration.

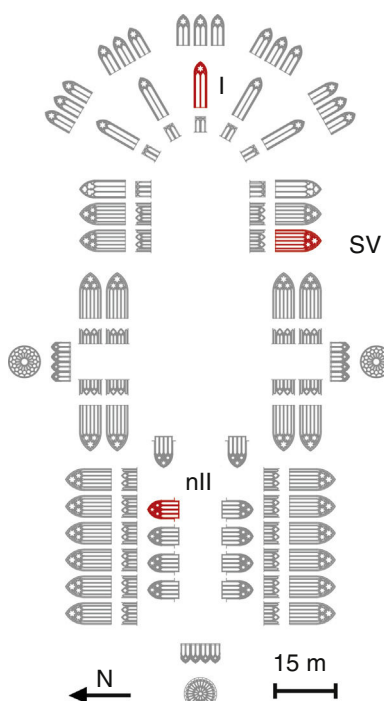


**Fig. 1 – Plan of the stained glass windows of the Cathedral of León. The fragments come from the windows marked in red.**

### Characterization techniques

The glass samples studied were characterized by the following techniques: optical microscopy (OM), scanning electron microscopy (SEM), energy dispersive X-ray microanalysis (EDS), X-ray fluorescence (XRF) spectrometry, VIS spectrophotometry and X-ray diffraction (XRD).

OM was carried out by a Leica MZ16 reflected light microscope equipped with a Leica DC300 camera.

SEM observations were undertaken by a Hitachi S-3400-N electron microscope, using acceleration voltages of 15 kV and both the secondary electrons mode (SE) and the backscattered electrons mode (BSE). Samples were EDS micro-analyzed on both surface and resin inlaid polished cross-section, using a carbon conductive coating deposited through a sputter coater Polaron SC7620. EDS micro-analyses were accomplished by a Bruker AXS XFlash Quantax 4010 spectrometer with energy resolution of 125 eV (Mn K $\alpha$ ) attached to the SEM equipment. EDS determinations with the theoretical inner pattern were obtained by using the ZAF method of correction and the Bruker Sprint 1.8 analytical software.

Semi-quantitative chemical analysis by XRF was carried out by a PANalytical Axios wavelength dispersed X-ray spectrometer equipped with a tube of rhodium of 4 kW and 60 kV. Analytical determinations were undertaken through the standard-less analytical software IQ+ (PANalytical) based on fundamental parameters from synthetic oxides and well-characterized natural minerals. In addition, Sheffield glass nos. 7 and 10 (Society of Glass Technology) are commonly used as internal routine control standards. Powder samples (1 g approx.) for bulk XRF analysis were prepared by grinding body glass fragments, with their most external surfaces removed by polishing, in an agate mortar. After that, pressed boric acid pellets were made, using a mixture of n-butylmethacrylate and acetone (10:90 wt.%) as binding medium. Just the samples L1, L2, L9, L10 and L11 presented enough mass to be analyzed by XRF. The other samples were micro-analyzed by EDS on polished cross-sections.

The color of the glass samples was characterized by visible spectrophotometry (VIS) with an Ocean Optics HR 4000 CG spectrophotometer. Spectra were recorded in the 250–1100 nm range on glass samples of approximately 1 mm thick obtained by polishing both sides of the samples to optical quality.

XRD measurements were collected with a Phillips X'Pert MPD diffractometer equipped with a copper X-ray tube. A current of 40 mA and a voltage of 45 kV were employed as tube settings. XRD data was collected between  $2\theta = 5^\circ$  and  $60^\circ$ .

## Results and discussion

### Chemical composition

The different interventions in the Cathedral of León throughout History increased the diversity of glass compositions present in the stained glass windows [21]. Brill classified the medieval glasses from the Cathedral of León in three different groups [24]. Type I and Type II are very similar one each other because they presented a high concentration of K<sub>2</sub>O (12–20 wt.%) and a moderate content of CaO (10–15 wt.%) and a

**Table 1 – Main characteristics of the glass samples studied.**

Sample	Color	Outdoor surface appearance	Indoor surface appearance	Location
L1	Light pink	Pits	Grisaille	nII
L2	Green	Pits, alteration crust	Grisaille, pits	I
L3	Red flash	Alteration crust	Pits	SV
L4	Yellow	Alteration crust	Pits	SV
L5	Blue	Deposits	Grisaille	SV
L6	Red flash	Alteration crust	Grisaille, pits	SV
L7	Pink	Alteration crust	Grisaille	SV
L8	Violet flash	Pits	Grisaille	Glassman boxes
L9	Greenish	Alteration crust, pits	Grisaille	Glassman boxes
L10	Yellow	Pits	Grisaille, putty	Undetermined
L11	Greenish	Dust	Grisaille	Undetermined

high content of MgO (5–10 wt.%) (Figs. 2 and 3a). The main difference between these two groups is the content of P<sub>2</sub>O<sub>5</sub>, which can be related with the ashes used for the glasses manufacture [24,30]. Glasses of Type I presented a concentration

of P<sub>2</sub>O<sub>5</sub> of 1–4 wt.%, while the glasses of Type II had around 4–5 wt.%. These types of glasses were manufactured between the 13th and the 14th centuries [24].

Glasses of Type III, possibly dated in 14th–15th centuries, had low silica content (lower than 50 wt.%) and high content of K<sub>2</sub>O and CaO (20–27 and 19–24 wt.%, respectively) with moderated percentages of MgO (~4 wt.%) (Fig. 2) [24]. Valle [26] identified a new group of glasses (Type IV) from the Renaissance (15th–16th centuries). These glasses presented a chemical composition similar to that of the Type III defined by Brill (Fig. 2), but with a high concentration of Al<sub>2</sub>O<sub>3</sub> (Fig. 3a). Carmona [12] identified another group of Renaissance glasses (Type V) with a very high content of SiO<sub>2</sub> and CaO (>55% and 12–26 wt.%, respectively), and a low content of K<sub>2</sub>O (6–11 wt.%) (Fig. 2). These groups also presented a very high concentration of Al<sub>2</sub>O<sub>3</sub> (2–4 wt.%) and low of MgO (< 2 wt.%) (Fig. 3a). Carmona [12,27] also analyzed Late-Medieval and Modern glasses with different chemical compositions (Fig. 3a).

The representation of Al<sub>2</sub>O<sub>3</sub>/SiO<sub>2</sub> vs. TiO<sub>2</sub>/Al<sub>2</sub>O<sub>3</sub> allows relating the composition of glasses with the mineralogy of the glassmaking sands [31]. As can be seen in Fig. 3b, the samples were divided according to the glass types previously defined, which provides solid evidence that each glass type presented different sources of raw materials or different production technology. Type I and Type II showed a high content of TiO<sub>2</sub>/Al<sub>2</sub>O<sub>3</sub>, which suggested the use of a silica source with high content of heavy minerals. However, Type III and Type IV had an oxide relation typical from Levantine Roman glasses, and then they suggest another kind of silica source [31]. It is also highlighted

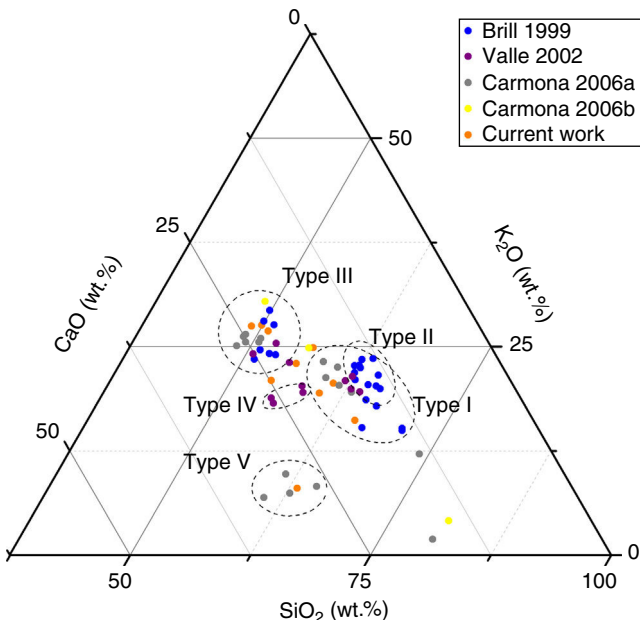


**Fig. 2 – Ternary representation of the glass compositions of the samples archaeometrically characterized in the current and previous works [12,25–27].**

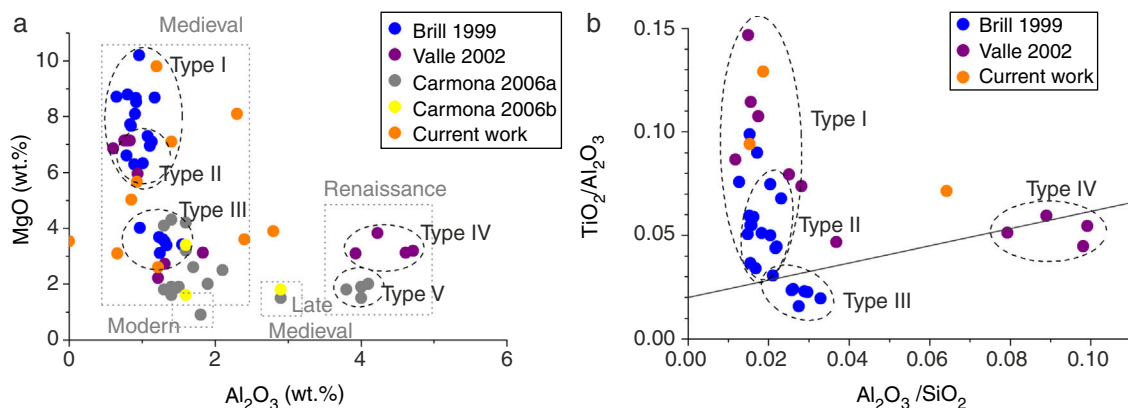


**Fig. 3 – Binary representation of (a) Al<sub>2</sub>O<sub>3</sub> vs. MgO (wt.%) and (b) Al<sub>2</sub>O<sub>3</sub>/SiO<sub>2</sub> vs. TiO<sub>2</sub>/Al<sub>2</sub>O<sub>3</sub>.**

**Table 2 – Chemical composition of the glass samples from the Cathedral of León analyzed by XRF and EDS spectrometries and normalized to 100 wt.%.**

Samples	XRF analyses					EDS analyses								
	L1	L2	L9	L10	L11	L1	L4	L5	L6	L7	L8	L9	L10	L11
Na <sub>2</sub> O	< d.l.	0.77	2.77	2.63	< d.l.	0.3	3.2	4.6	0.6	3.1	0.4	3.2	3.9	1.3
MgO	3.10	2.60	5.66	5.03	3.54	3.9	8.1	9.8	3.9	7.1	3.6	8.5	6.7	4.9
Al <sub>2</sub> O <sub>3</sub>	0.66	1.22	0.93	0.85	< d.l.	0.7	2.3	1.2	2.8	1.4	2.4	0.9	1.1	4.2
SiO <sub>2</sub>	50.41	45.68	49.92	55.48	57.32	44.0	45.5	46.3	43.6	44.9	44.7	41.0	47.7	45.4
P <sub>2</sub> O <sub>5</sub>	0.98	0.62	4.64	3.65	1.94	1.0	2.8	4.2	1.1	3.6	1.1	4.8	3.9	2.3
SO <sub>2</sub>	0.30	0.23	0.19	0.07	0.14	0.4	0.3	0.2	0.1	< d.l.	< d.l.	0.1	< d.l.	< d.l.
Cl <sup>-</sup>	0.07	0.06	0.39	0.60	0.22	< d.l.	0.5	0.5	< d.l.	0.5	< d.l.	0.5	0.7	0.3
K <sub>2</sub> O	19.47	24.1	16.91	13.75	7.26	22.2	20.0	15.0	24.5	18.5	24.7	21.0	17.0	9.6
CaO	23.09	19.91	15.23	15.77	25.89	25.4	14.9	15.9	21.1	17.1	20.2	17.3	17.1	28.5
TiO <sub>2</sub>	< d.l.	< d.l.	0.12	0.08	0.43	0.8	< d.l.	< d.l.	0.2	< d.l.	< d.l.	0.2	< d.l.	0.8
MnO	1.02	0.78	2.04	1.25	1.24	1.0	1.3	1.3	0.9	2.1	1.1	2.3	1.2	1.2
Fe <sub>2</sub> O <sub>3</sub>	0.25	3.20	0.61	0.61	1.42	0.7	1.1	1.1	1.0	1.0	0.9	0.3	0.9	1.5
CoO	< d.l.	< d.l.	< d.l.	< d.l.	0.04	< d.l.	< d.l.	< d.l.	< d.l.	< d.l.	< d.l.	< d.l.	< d.l.	< d.l.
CuO	< d.l.	0.03	0.27	< d.l.	< d.l.	< d.l.	< d.l.	< d.l.	< d.l.	< d.l.	< d.l.	< d.l.	< d.l.	< d.l.
ZnO	0.05	0.05	0.07	0.07	0.02	< d.l.	< d.l.	< d.l.	< d.l.	< d.l.	< d.l.	< d.l.	< d.l.	< d.l.
As <sub>2</sub> O <sub>3</sub>	< d.l.	< d.l.	< d.l.	< d.l.	0.06	< d.l.	< d.l.	< d.l.	< d.l.	< d.l.	< d.l.	< d.l.	< d.l.	< d.l.
Rb <sub>2</sub> O	0.08	0.12	0.03	0.03	0.02	< d.l.	< d.l.	< d.l.	< d.l.	< d.l.	< d.l.	< d.l.	< d.l.	< d.l.
SrO	0.13	0.13	0.08	0.07	0.09	< d.l.	< d.l.	< d.l.	< d.l.	< d.l.	< d.l.	< d.l.	< d.l.	< d.l.
ZrO	< d.l.	0.02	< d.l.	0.14	0.04	< d.l.	< d.l.	< d.l.	< d.l.	< d.l.	< d.l.	< d.l.	< d.l.	< d.l.
BaO	0.26	0.21	0.14	0.45	0.29	< d.l.	< d.l.	< d.l.	< d.l.	< d.l.	< d.l.	< d.l.	< d.l.	< d.l.
PbO	0.14	0.26	< d.l.	< d.l.	< d.l.	< d.l.	< d.l.	< d.l.	< d.l.	0.2	0.7	1.0	< d.l.	< d.l.
Bi <sub>2</sub> O <sub>3</sub>	< d.l.	< d.l.	< d.l.	< d.l.	0.04	< d.l.	< d.l.	< d.l.	< d.l.	< d.l.	< d.l.	< d.l.	< d.l.	< d.l.

< d.l.: lower than the detection limit.

the very high content of Al<sub>2</sub>O<sub>3</sub> in comparison with the SiO<sub>2</sub> content in the Type IV (Fig. 3b), which reflected the presence of feldspar in the glassmaking sands or an intentioned addition of Al<sub>2</sub>O<sub>3</sub> to stabilize the glass [26].

The analytical study of the samples characterized in this study showed that all the fragments were potash-lime silicate glasses (Table 2), and they were integrated in the medieval glass types previously defined (Fig. 2). Even the fragment L11, from Renaissance chronology, had a chemical composition similar to the glasses from Type V (Fig. 2) from the same chronology; nevertheless, the Al<sub>2</sub>O<sub>3</sub> content is lower than the detection limit of the equipment (Table 2).

#### Chromatic study

Glass fragments showed a great variety of colors. Nevertheless just the samples L1, L2, L8, L9, L10 and L11 were large enough

to be chromatically characterized. The most common chromophore found in the glasses was iron, which is an impurity of the glassmaking sand. The majority of the samples presented the iron ions bands join with the other chromophores bands; just the sample L10 presented the characteristic bands of the Fe<sup>2+</sup> (~1028 nm) and Fe<sup>3+</sup> (386 and 419 nm) (Fig. 4a).

Cobalt ions have a high molar extinction coefficient that, even in a very low concentration, yields blue colored glasses. The samples L2, L9 and L11 presented simultaneously the bands of Co<sup>2+</sup> ions and of the redox pair Fe<sup>3+</sup>/Fe<sup>2+</sup>, which result in a greenish hue of the glass (Fig. 4b).

The main chromophore in the sample L1, with a light pink hue, was assigned to Mn<sup>3+</sup> ions (Fig. 5a). This color is the most common in the representation of the human skin. The sample L8 is a flash glass composed by a purple glass over a greenish glass. The chromatic characterization of the ensemble presented the bands of the Fe<sup>3+</sup> ions, the very intense band of

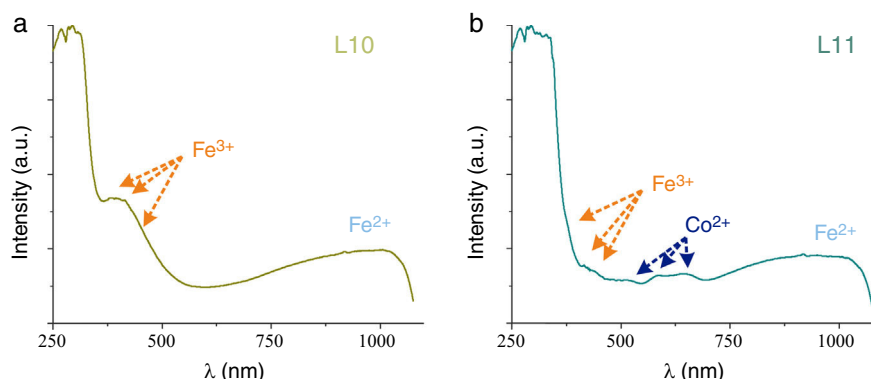


Fig. 4 – VIS absorption spectra from samples: (a) L10 and (b) L11.

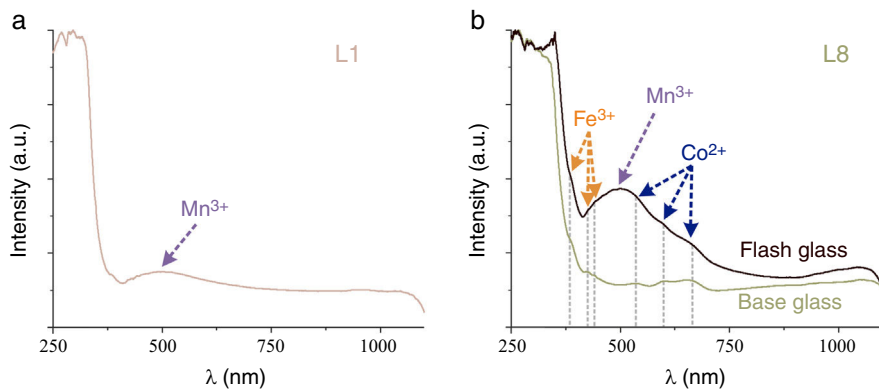
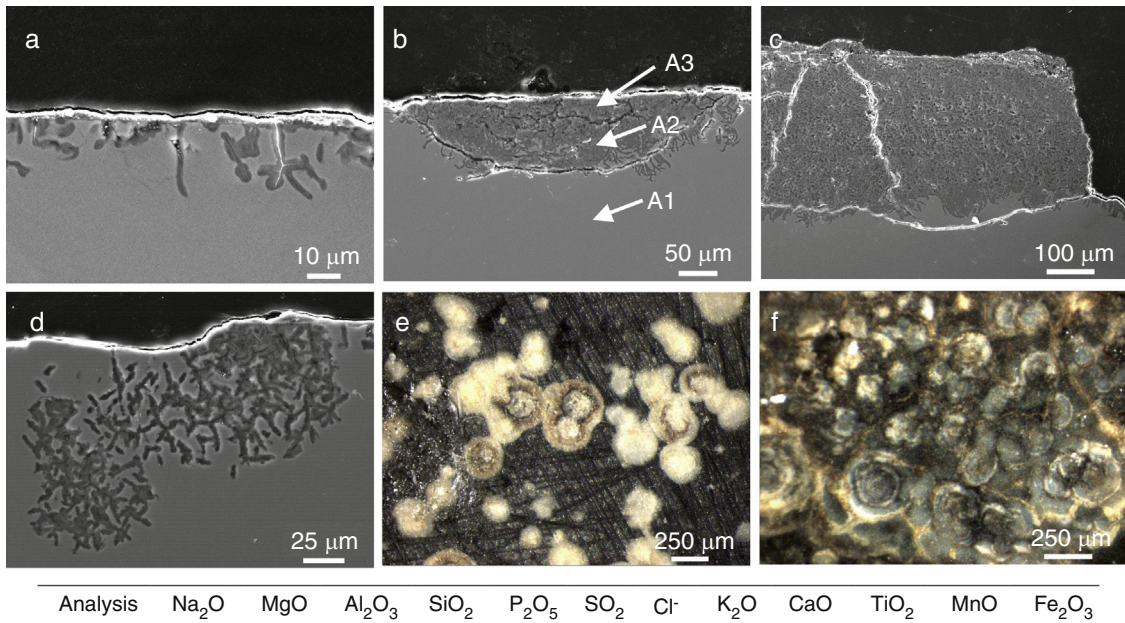


Fig. 5 – VIS absorption spectra from samples: (a) L1 and (b) L8.



Analysis	Na <sub>2</sub> O	MgO	Al <sub>2</sub> O <sub>3</sub>	SiO <sub>2</sub>	P <sub>2</sub> O <sub>5</sub>	SO <sub>2</sub>	Cl <sup>-</sup>	K <sub>2</sub> O	CaO	TiO <sub>2</sub>	MnO	Fe <sub>2</sub> O <sub>3</sub>
A1	3.2	8.5	0.9	41.0	4.8	0.1	0.5	21.0	17.3	0.2	2.3	0.3
A2	1.2	3.4	1.3	67.7	6.9	0.6	0.4	5.3	10.0	0.4	2.0	1.0
A3	0.6	1.4	1.6	71.1	4.1	1.7	0.3	1.8	10.0	0.5	5.4	1.6

Fig. 6 – SEM micrographs in cross section of (a) fissures in the sample L8, (b) a pit in advanced stage of alteration in the sample L9, (c) alteration layer in the sample L9, (d) a pit in an early stage of alteration in the sample L10. Binocular microscope image of (e) isolated pits in the outdoor surface of the sample L9, (f) interconnected pits in the outdoor surface of the sample L10. The enclosed table displays EDS microanalyses results (wt.%).

the Mn<sup>3+</sup> and two of the three characteristic bands of the Co<sup>2+</sup> ions (Fig. 5b). However, the base glass showed just the bands of Co<sup>2+</sup> and Fe<sup>3+</sup> ions, responsible of the greenish hue.

#### Surface alterations

Glass samples presented a completely different surface alteration depending on their chemical composition, their indoor/outdoor surface and their location in the cathedral.

The sample L8 presented small fissures of ~25 μm in depth in its outdoor surface (Fig. 6a). Some areas, with a dark color in the SEM images, were identified such as dealkalinization channels formed by the hydrolytic attack of the water and the lixiviation of alkaline and alkaline-earth ions from the glass (Reactions (1)–(3)). The water in the surface can be filtered through these channels spreading the attack toward the bulk glass (Fig. 6d).

A more intense attack in these areas can form pits, which usually have a semispherical front (Fig. 6b and e). The chemical

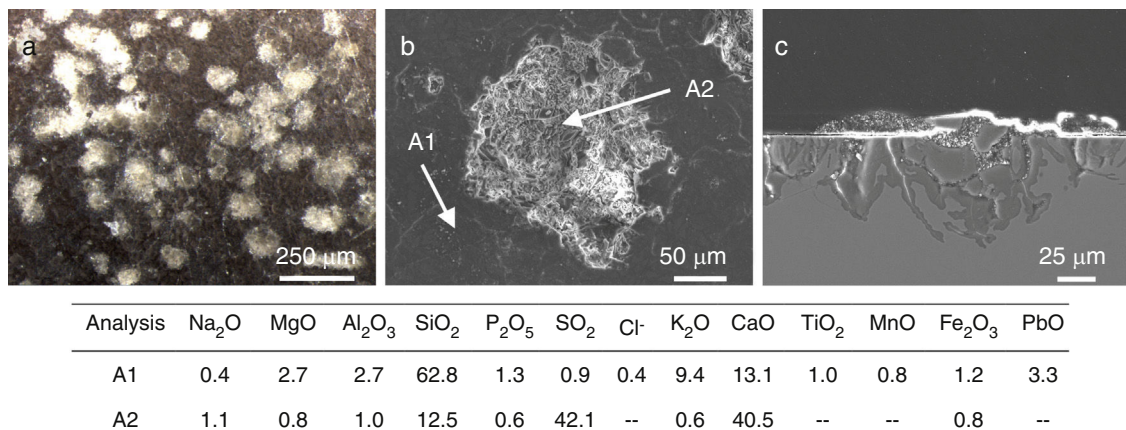


**Fig. 7 – (a) Binocular microscope image of the pits in the outdoor surface of the sample L1. SEM micrographs of (b) an irregular pit filled with crystalline deposits, (c) cross section of an irregular pit. The enclosed table displays EDS microanalyses results (wt.%).**

analysis in these areas showed an advanced dealkalination process (Fig. 6b, analyses A1, A2 and A3). The K<sub>2</sub>O content decreased progressively from 21.0 wt.% in the unaltered glass to 1.8 wt.% in the most advanced corrosion area. CaO has been partially lixiviated. On the contrary, SiO<sub>2</sub> has been relatively increased up to 71.1 wt.% in the most altered area (Fig. 6b, analysis A3).

The pits interconnection and/or the homogeneous alteration of the glass surface can produce a continuous alteration front (Fig. 6c). The fissures formed between both altered and unaltered areas can induce mechanical detachments which form craters on the glass surface (Fig. 6c and f).

The sample L1 presented different alteration pathologies. It showed an irregular surface with numerous craters filled with crystalline deposits in the fragment outdoor surface (Fig. 7a and b). The growth of crystals inside the fissures favored the detachment of the altered glass fragments that generated irregular craters (Fig. 7c). These crystals were formed by the chemical reaction of the ions lixiviated from the bulk glass and the atmospheric pollutants (SO<sub>2</sub>, CO<sub>2</sub>, NO<sub>x</sub>), dissolved in the surface water, and filtered through the fissures (Fig. 7, analyses A1 and A2; Reactions (7)–(9)) [12].

There is a direct relationship between the pit formation mechanism and the location of the samples. The pits due to dealkalination were mainly formed in the glasses from the Glassman boxes, which were retired in the 19th century. While the glasses exposed until nowadays presented irregular pits with crystalline deposits, mainly CaSO<sub>4</sub>, due to the synergic effect of the humidity and the atmospheric pollution near the cathedral.

Both alteration mechanisms were identified in the sample L3. The red flash layer in the indoor surface was lost as result of the pits formation (Fig. 8), and the outdoor surface was completely covered by a degradation crust. This sample was probably located inside-out. The interconnected pits were formed by dealkalination in the supposed outdoor surface (current indoor surface) until the 19th century; then, the panel would be changed and the current outdoor surface was

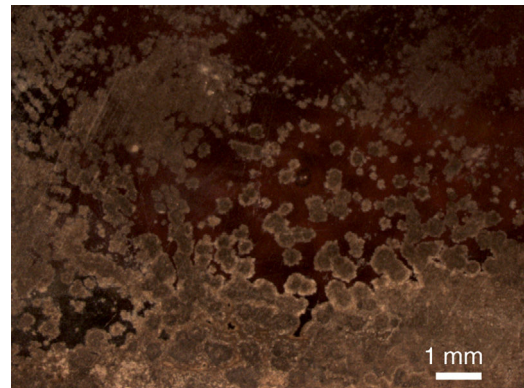


**Fig. 8 – Binocular microscope image of the pits in the red flash layer on the sample L3.**

exposed to the environmental pollution being completely covered by crystalline deposits. Such a change of glasses and/or panels was a common practice in the restorations before the 20th century [32].

Six glasses (L2, L3, L4, L6, L7 and L9) had a homogeneous crust in their outdoor surface as consequence of a long contact with the polluted environment. The XRD analysis of the alteration crust of the sample L7 showed that it was formed by gypsum (CaSO<sub>4</sub>·2H<sub>2</sub>O) as the main crystalline phase, a low proportion of quartz (SiO<sub>2</sub>) from the environmental dust [33], and iron or iron silicon (Fe<sub>0.9</sub>Si<sub>0.1</sub>) from the corrosion of the metallic elements of the stained glass windows [28] (Fig. 9). A reddish layer with a high content of Fe<sub>2</sub>O<sub>3</sub> (Fig. 10a and b, analysis A2) was also detected upon the alteration crust (Fig. 10c) in the areas near to these metallic elements.

In general, the grisaille protect the glass surface and prevent its alteration (Fig. 11a) [27]. However, when the grisaille is altered, the rain or condensation water can be filtered through the fissures favoring the local degradation of the subjacent glass (Fig. 11b and c) or the general glass damage (Fig. 11d). The

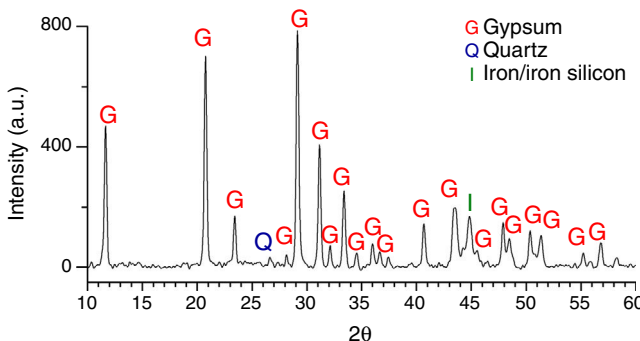


**Fig. 9 – XRD pattern of the corrosion crust on the surface of the sample L7.**

samples L6 and L8 showed pits in the indoor surface under the grisailles.

Finally, a slight enrichment in MnO was detected in the altered areas of the glasses L6 and L9 (Fig. 6c, analyses A1, A2 and A3; Fig. 12, analyses A1, A2 and A3). MnO was also detected in the alteration crust of the samples L3, L4, L5 and L7. The grisaille showed a low content of manganese (Fig. 12a, analysis A3). The MnO enrichment can be connected with the browning process in the glasses, in which the manganese ions from the glass would precipitate as  $MnO_2$  [34]. This process depends on the environmental conditions and is favored by humid and acid environments [35].

#### Relation between chemical composition and alteration pathologies

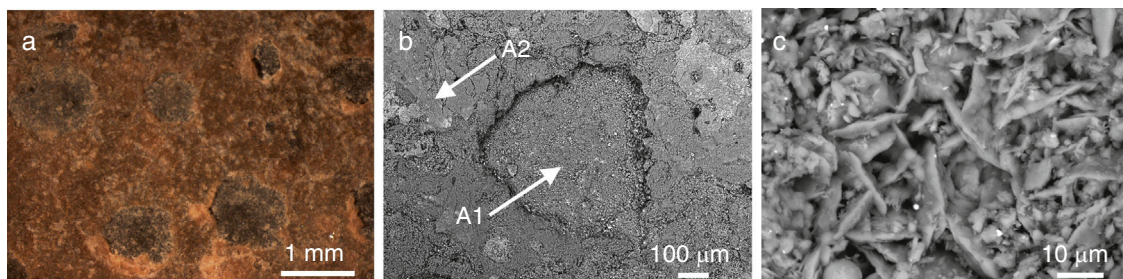
According to the Bettembourg classification [36], which related the alteration pathologies in medieval glasses with the chemical composition, the samples L10 and L11 should be stable glasses because they had content of  $SiO_2 > 54$  wt.% and  $K_2O < 14$  wt.%; the glass fragments L5 and L9 should be covered by pits, and the rest of the samples should present a uniform altered surface because the glasses presented a high content

of  $K_2O$  (Fig. 13). In fact, all the samples showed surface alterations, preferentially in the outdoor surface of the glasses instead of the fragment L11 (Table 1). All the glasses with a degradation crust upon the outdoor surface (L2, L3, L4, L6, L7 and L9) had a relation  $K_2O/CaO > 1$ , unless the sample L8 which presented isolated deposits. This fact highlights the important relationship between the chemical composition and the degradation state, although other factors such as the microclimate of each location influenced the alteration process as well.

The alteration pathologies of the Type I, II and III from the Cathedral of León were previously analyzed by Goldkuhle [37]. The samples from the 15th century presented brownish alteration layers on the outdoor side of the glasses, however the 13th century glasses (Type I and II) showed different alteration pathologies, e.g. isolated pits and uniform crusts [37]. The different alteration process was connected with the chemical composition of the glasses. The majority of the glasses identified by Brill showed a relation  $K_2O/CaO > 1$  ( $1.3 \pm 0.2$  for Type I,  $1.6 \pm 0.2$  for Type II and  $1.1 \pm 0.2$  for Type III), indicating the low stability of these glasses, particularly of the Type III which present a lower content of  $SiO_2$  (Fig. 13). Goldkuhle highlighted the good state of conservation of the stained glass windows 1 and 31, located in the west façade and protected by the towers [37], however the relatively high content of  $SiO_2$  of the sample 6001 from the window 1 could also diminish the alteration rate [25].

Valle et al. detected gypsum ( $CaSO_4 \cdot 2H_2O$ ), bassanite ( $CaSO_4 \cdot 0.5H_2O$ ) and a mix of both in the corrosion crust on both sides of the glasses; however the crystallization was lesser on the indoor surface due to the softer impact of the environmental factors [26]. Renaissance glasses presented higher chemical stability, which was attributed to their relatively high content of  $Al_2O_3$  and to their relation  $K_2O/CaO < 1$  (Fig. 13).

The medieval glasses analyzed by Carmona et al. presented craters and corrosion crusts on the outdoor surface, and thin crusts, pits or no-alteration pathologies in the indoor surface [12]. Most of these samples presented relation  $K_2O/CaO > 1$



Analysis	MgO	$Al_2O_3$	$SiO_2$	$P_2O_5$	$SO_2$	$Cl^-$	$K_2O$	CaO	MnO	$Fe_2O_3$	PbO
A1	0.7	1.0	19.5	0.6	28.2	--	1.8	35.6	--	7.6	4.9
A2	1.6	3.6	44.7	2.1	3.6	0.3	3.6	4.5	0.7	33.0	2.2

**Fig. 10 – (a) Binocular microscope image of the reddish layer upon the outdoor surface of the sample L2. SEM micrographs of (b) the reddish layer upon the alteration crust, (c) deposits inside one crater in the reddish layer. The enclosed table displays EDS microanalyses results (wt.%).**

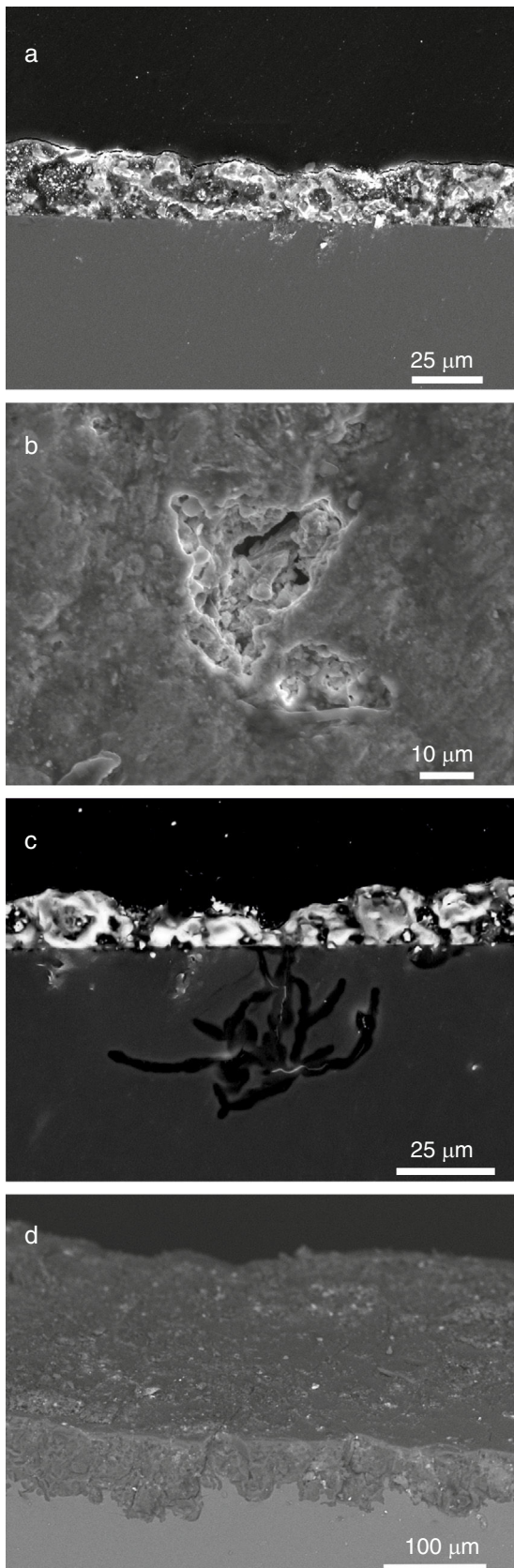


**Fig. 11 – SEM micrograph of (a) a consolidated grisaille in the sample L8, (b) a fissure in the grisaille of sample L8, (c) dealkalinization channels in the glass of sample L8, (d) general alteration of the glass of sample L6.**

(Fig. 13), and showed a good state of conservation compared to other similar glasses. This can be explained because the first set of fragments were retired from the corresponding stained glass windows in the 19th century and were kept in the Glassman boxes until nowadays. Furthermore some Renaissance glasses presented thick corrosion layers on the outdoor surface and thin layers on the indoor side, even with relation  $K_2O/CaO \sim 0.3$ . This severe alteration could be related to the exposition of such Renaissance glasses throughout the 20th century, when the concentration of environmental pollution due to charcoal stoves and transports was higher [12]. The 19th century glasses presented a good state of conservation due to their high content of  $SiO_2$  (>64 wt.%) and their relation  $K_2O/CaO < 1$ , mainly in the sample 28 [12].

Finally, the influence of the microclimate in each location was monitored with glass sensors patented by the Fraunhofer-Institut für Silicatforschung ISC (Germany) [38]. The sensors demonstrated that the glasses from the North façade presented a more intense alteration than glasses from the South façade [20,39]. Even the alteration of the glass sensors in the lower part of the stained glass windows was similar in all orientations and lower than those of sensors located in the upper part of the windows [39]. The architecture of the building could have had some influence under each microclimate, because in the lower part of the façade the structure is more open than in the upper part and favors the washing of the surface products by the rainwater minimizing the damage induced by the stationary conditions (Reactions (4)–(6)) [9].

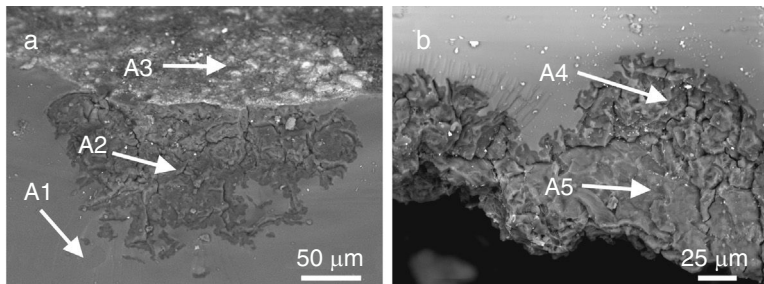
Currently a protective glazing system has been installed as a preventive conservation strategy to protect the stained glass windows from the atmospheric weathering (rain, wind, pollution, etc.). This protective system was installed at about 6 cm from the original stained windows. The natural ventilation was achieved by slots of about 1–2 cm on the bottom and the top of the window toward the building indoors [39]. The environmental monitoring by means of glass sensors proved the efficacy of the protective glazing system against the alteration of the original stained glass windows [39].

## Conclusions

The glasses from the Cathedral of León can be classified into five groups as a function of their chemical composition. These groups represent the glasses from different chronologies, in which different raw materials sources or different production technologies were used.

As concerns the chromatic characterization, the redox pair  $Fe^{3+}/Fe^{2+}$  was detected in all the samples, since iron ions are a common impurity of the sands used as glass raw materials. The chromophores  $Co^{2+}$  and  $Mn^{3+}$ , usual in medieval times, were also detected.

Finally, the direct relationship between the glass degradation state and the environment was verified. The samples from the Glassman boxes, retired during the 19th century, presented pits due to the dealkalinization of the glasses. However, those glasses exposed during the last century presented crystalline deposits, mainly  $CaSO_4$ , on the surface and in the fissures as a consequence of the atmospheric pollution of León city during the 20th century. In some glasses the manganese enrichment,



Analysis	Na <sub>2</sub> O	MgO	Al <sub>2</sub> O <sub>3</sub>	SiO <sub>2</sub>	P <sub>2</sub> O <sub>5</sub>	SO <sub>2</sub>	Cl <sup>-</sup>	K <sub>2</sub> O	CaO	MnO	Fe <sub>2</sub> O <sub>3</sub>	CuO	PbO
A1	0.6	3.9	2.8	43.6	1.1	0.1	--	24.5	21.1	0.9	1.0	--	0.2
A2	--	1.0	4.6	53.9	0.6	0.3	--	3.5	24.2	3.0	2.4	--	6.6
A3	--	0.9	2.4	17.4	0.9	--	0.5	3.2	8.2	0.8	38.4	5.1	22.3
A4	0.1	0.6	4.5	65.7	1.5	0.1	--	4.5	17.4	2.6	1.5	--	1.6
A5	--	0.6	5.7	71.4	2.0	0.3	--	2.6	11.4	3.3	1.6	--	1.3

Fig. 12 – SEM-BSE micrographs in the fresh fracture of the altered area (a) under the grisaille, (b) in the outdoor surface, of sample L6. The enclosed table displays EDS microanalyses results (wt.%).

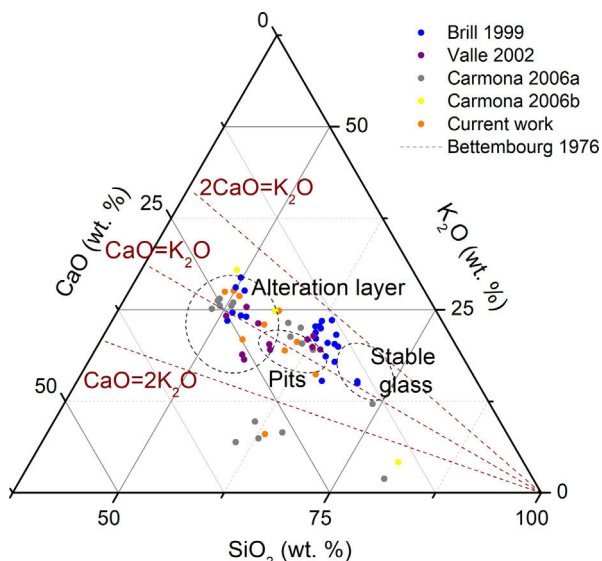


Fig. 13 – Ternary representation of the glass compositions of the samples characterized in the current and previous works [12,25–27] to compare their degradation pathologies [36].

connected with the browning alteration, was detected in the alteration layer and the corrosion crust.

## Acknowledgments

The author acknowledges to Mrs. Ángeles Robles (Vidrieras Catedral de León S.L.) and to Mr. José Antonio Campo Muñoz (ESOCA S.L.) the facilities provided to accomplish this research and to the CERVITRUM research group (CCHS-

CSIC, Madrid) for their help during the study. The author also acknowledges the partial funding of the program GEOMATERIALES 2-CM ref. S2013/MIT-2914 and a post-doctoral fellowship from the Ministério de Ciência e Tecnologia de Portugal (ref. SFRH/BPD/108403/2015), as well as professional support from TechnoHeritage (Network of Science and Technology for the Conservation of Cultural Heritage).

## REFERENCES

- [1] T. Palomar, M. García Heras, M.Á. Villegas, Archaeological and historical glasses: a bibliometric study, *Bol. Soc. Esp. Ceram.* V 48 (2009) 187–194.
- [2] T. Palomar, La interacción de los vidrios históricos con medios atmosféricos, acuáticos y enterramientos (Ph.D. thesis), Universidad Autónoma de Madrid, 2013 <https://repositorio.uam.es/handle/10486/12962>.
- [3] R.A. Lefèvre, M. Grégoire, M. Derbez, P. Ausset, Origin of sulphated grey crusts on glass in polluted urban atmosphere: stained glass windows of Tours Cathedral (France), *Glass Sci. Technol.* 71 (1998) 75–80.
- [4] I. Munier, R. Lefèvre, R. Losno, Atmospheric factors influencing the formation of neocrystallisations on low durability glass exposed to urban atmosphere, *Glass Technol.* 43 (C) (2002) 114–124.
- [5] O. Favez, H. Cachier, A. Chabas, et al., Crossed optical and chemical evaluations of modern glass soiling in various European urban environments, *Atmos. Environ.* 40 (2006) 7192–7204, <http://dx.doi.org/10.1016/j.atmosenv.2006.06.022>.
- [6] T. Lombardo, R.A. Lefèvre, A. Chabas, et al., Characterisation of particulate matter deposition inducing soiling of modern glass, in: *Air Pollution and Cultural Heritage*, A.A. Balkema Publishers, Londres, 2004, pp. 209–214.
- [7] T. Lombardo, A. Chabas, R.A. Lefèvre, Weathering of float glass exposed outdoors in an urban area, *Glass Technol.* 46 (2005) 271–276.

- [8] T. Lombardo, A. Chabas, A. Verney-Carron, et al., Physico-chemical characterisation of glass soiling in rural, urban and industrial environments, *Environ. Sci. Pollut. Res.* 21 (2014) 9251–9258, <http://dx.doi.org/10.1007/s11356-014-2853-4>.
- [9] J.M. Fernández Navarro, *El vidrio*, Consejo Superior de Investigaciones Científicas, Sociedad Española de Cerámica y Vidrio, Madrid, 2003.
- [10] M. Perez y Jorba, J.P. Dallas, R. Collongues, et al., Etude de l'altération des vitraux anciens par microscopie électronique à balayage et microsonde, *Silic. Ind.* 43 (1978) 89–99.
- [11] K. Bange, O. Anderson, F. Rauch, et al., Multi-method characterization of soda-lime glass corrosion. Part 2. Corrosion in humidity, *Glass Sci. Technol.* 75 (2002) 20–33.
- [12] N. Carmona, M.A. Villegas, J.M. Fernandez Navarro, Characterisation of an intermediate decay phenomenon of historical glasses, *J. Mater. Sci.* 41 (2006) 2339–2346, <http://dx.doi.org/10.1007/s10853-005-3948-6>.
- [13] T. Palomar, A. Chabas, D.M. Bastidas, et al., Effect of marine aerosols on the alteration of silicate glasses, *J. Non-Cryst. Solids* 471 (2017) 328–337, <http://dx.doi.org/10.1016/j.jnoncrysol.2017.06.013>.
- [14] M. Schreiner, M. Grasserbauer, P. March, Quantitative NRA and SIMS depth profiling of hydrogen in naturally weathered medieval glass, *Fresen. Z. Anal. Chem.* 331 (1988) 428–432, <http://dx.doi.org/10.1007/BF00481921>.
- [15] M. Aulinás, M. Garcia-Valles, D. Gimeno, et al., Weathering patinas on the medieval (S. XIV) stained glass windows of the Pedralbes Monastery (Barcelona, Spain), *Environ. Sci. Pollut. Res.* 16 (2009) 443–452, <http://dx.doi.org/10.1007/s11356-008-0078-0>.
- [16] M. Vilarigues, P. Redol, A. Machado, et al., Corrosion of 15th and early 16th century stained glass from the Monastery of Batalha studied with external ion beam, *Mater. Charact.* 62 (2011) 211–217, <http://dx.doi.org/10.1016/j.matchar.2010.12.001>.
- [17] D. Watkinson, L. Weber, K. Anheuser, Staining of archaeological glass from manganese-rich environments, *Archaeometry* 47 (2005) 69–82, <http://dx.doi.org/10.1111/j.1475-4754.2005.00188.x>.
- [18] W. Müller, H. Pouillon, G. Bochynek, H. Mehner, Extreme dunkelung von glasmalereien, *Glastech. Ber.* 59 (1986) 96–102.
- [19] J.M. Fernández Navarro, Procesos de alteración de las vidrieras medievales: Estudio y tratamientos de protección, *Mater. Construcc.* (1996) 5–26.
- [20] A. Robles Robles, Las vidrieras de la Catedral de León: Estado de conservación. Métodos aplicados para su conservación y protección, in: Jornadas nacionales sobre restauración y conservación de vidrios, Fundación Centro Nacional del Vidrio, Real Fábrica de Cristales de La Granja, San Ildefonso, Segovia, Spain, 1999, pp. 65–78.
- [21] M. Gómez Rascon, Catedral de León. Las vidrieras. El simbolismo de la luz, Edilesa, León, 2000, pp. 149–151.
- [22] J. Arlington, Catedral de León: seven centuries of stained glass, *Stain. Glass Q.* 90 (1995) 304–308.
- [23] B. Corral Hospital, Vidrieras de la Catedral de León (Bachelor Project), Universidad de Valladolid, 2015, [https://uvadoc.uva.es/bitstream/10324/16362/1/TFG\\_F\\_2015\\_100.pdf](https://uvadoc.uva.es/bitstream/10324/16362/1/TFG_F_2015_100.pdf).
- [24] R.H. Brill, S. Weintraub, Chemical analysis of some stained glass windows in León Cathedral, in: Proceedings of the 16th International Congress of Glass, 1992, pp. 143–149.
- [25] R.H. Brill, Chemical Analyses of Early Glasses, The Corning Museum of Glass, Corning, New York, 1999.
- [26] F.J. Valle, P. Ortega, L. Pascual, et al., Chemical composition of Medieval stained glasses from the Cathedral of León (Spain), *Glass Sci. Technol.* 75 (2002) 152–157.
- [27] N. Carmona, M.A. Villegas, J.M. Fernandez Navarro, Study of glasses with grisailles from historic stained glass windows of the cathedral of Leon (Spain), *Appl. Surf. Sci.* 252 (2006) 5936–5945, <http://dx.doi.org/10.1016/j.apsusc.2005.08.023>.
- [28] J. Peña-Poza, T. Palomar, M. García-Heras, M.A. Villegas, Estudio y estudio de conservación de elementos metálicos de vidrieras de la Catedral de León, *Rev. Metal.* 46 (2010) 260–273, <http://dx.doi.org/10.3989/revmetalm.0960>.
- [29] M.A. Castro, F.J. Pereira, A.J. Aller, D. Littlejohn, Spectrometric investigation of the weathering process affecting historical glasses of León Cathedral, Spain, *Atmos. Environ.* 98 (2014) 41–49, <http://dx.doi.org/10.1016/j.atmosenv.2014.08.017>.
- [30] C.M. Jackson, J.W. Smedley, Medieval and post-medieval glass technology: melting characteristics of some glasses melted from vegetable ash and sand mixtures, *Glass Technol.* 45 (2004) 36–42.
- [31] N. Schibille, A. Sterrett-Krause, I.C. Freestone, Glass groups, glass supply and recycling in late Roman Carthage, *Archaeol. Anthropol. Sci.* (2016) 1–19, <http://dx.doi.org/10.1007/s12520-016-0316-1>.
- [32] A. Revuelta Bayod, La restauración de las vidrieras de la catedral de León en el siglo XIX: «El Árbol de Jessé», Espacio, tiempo y forma. Serie VII, Historia del Arte 20–21, 2007–2008, pp. 203–227.
- [33] P. Čupr, Z. Flegrová, J. Franců, et al., Mineralogical, chemical and toxicological characterization of urban air particles, *Environ. Int.* 54 (2013) 26–34, <http://dx.doi.org/10.1016/j.envint.2012.12.012>.
- [34] O. Schalm, K. Proost, K. De Vis, et al., Manganese staining of archaeological glass: the characterization of Mn-rich inclusions in leached layers and a hypothesis of its formation, *Archaeometry* 53 (2011) 103–122, <http://dx.doi.org/10.1111/j.1475-4754.2010.00534.x>.
- [35] T. Palomar, J.F. Conde, M. García-Heras, M.A. Villegas, El fenómeno del enmarramiento en las vidrieras de la Catedral de León, in: Proceedings of the 18th International Meeting on Heritage Conservation, Granada, 2011, pp. 239–242.
- [36] J.M. Bettembourg, Composition et altération des verres de vitraux anciens, *Verres Réfract.* 30 (1976) 36–42.
- [37] D. Goldkuhle, Selección de fenómenos de corrosión en las muestras de la Catedral de León, in: Conservación de vidrieras históricas: análisis y diagnóstico de su deterioro, Restauración, The Getty Conservation Institute, Los Angeles, 1997, pp. 159–164.
- [38] D.R. Fuchs, H. Römhild, H. Schmidt, Glass-sensors: assessment of complex corrosive stresses in conservation research, *MRS Proc.* 185 (2011), <http://dx.doi.org/10.1557/PROC-185-239>.
- [39] H. Römhild, Evaluation of protective glazing systems, *e-Preserv. Sci.* 1 (2004) 1–8.